

A Look-ahead Car Following Scheme for Efficient Driving on Urban Roads

M. A. S. Kamal* K. Hashikura* T. Hayakawa** T. Ogitsu*
K. Yamada* J. Imura**

* *Division of Mechanical Science and Technology, Graduate School of
Science and Technology, Gunma University, Kiryu 376-8515, Japan.*
(Corresponding Author M. A. S. Kamal, e-mail: maskamal@ieee.org)

** *School of Engineering, Tokyo Institute of Technology, Tokyo
152-8552, Japan.*

Abstract: For safe and efficient driving of a vehicle on urban roads, it is essential to analyze the trends of the vehicles ahead to take early measures in changing traffic situations. Existing efficient driving systems based on optimal car following compute the vehicle control input by solving an optimization problem over a prediction horizon, and at the expense of large computation cost, they provide significant improvement in traffic flows and fuel consumption. This paper proposes a look-ahead car following scheme, which can take anticipatory driving decisions with negligible computation cost, for efficient driving of a vehicle. Specifically, at first, the distinctive features of an optimal car following scheme over traditional car following of a human driver are investigated. Then, based on the features observed, a look-ahead car following scheme is formulated that can partly reflect the desired driving characteristics of the optimal car following scheme. The proposed scheme extends a traditional car following model by incorporating the predicted state of the preceding vehicle in a restricted look-ahead horizon. Finally, the proposed look-ahead car following scheme is evaluated in typical urban traffic scenarios, and the observed driving characteristics and performances are compared.

Keywords: Car following model, model predictive control, eco-driving.

1. INTRODUCTION

Improving safety, energy efficiency and traffic flows on urban roads are major demands as the number of vehicles on worldwide road-networks has been increasing. Various physical factors affect fuel consumption of vehicles, e.g., engine characteristics, powertrain system and vehicle structure related to aerodynamic drag and weather conditions. However, it has been revealed from various studies and experiments that the energy consumption of a vehicle is highly influenced by driving behavior (Berry, 2010; Knowles et al., 2012).

Microscopic human driving behavior is described by a car following model, which prescribes control acceleration according to the instantaneous driving context, e.g., presence and states of a vehicle in the front. A variety of car following models were developed and their behavioral aspects were well studied (Brackstone and McDonald, 1999). Some widely used ones include Gipps model (Gipps, 1981), optimal velocity model (OVM) (Bando et al., 1995), intelligent driver model (IDM) (Treiber et al., 2000). These models can approximately replicate human driving behavior related to the longitudinal motion of a vehicle in any traffic flow conditions.

Adaptive cruise control (ACC) based on a traditional control algorithm or cooperative ACC (CACC) are the advanced car following schemes developed for semi-automated vehicles. Taking a short gap between the ve-

hicles, these schemes improve the traffic capacity and flow performances (Davis, 2004; Kesting et al., 2008). Both ACC and traditional car following models are not energy efficient, and they may cause shock-waves or congestion in the traffic due to the presence of disturbances in dense traffic. Particularly, vehicles with these driving schemes often make aggressive braking due to the lack of traffic anticipation. Furthermore, they exhibit delayed or slow departure from a queue at an intersection, and such behavior causes reduction of the effective green time or the capacity of the intersection (Koonce et al., 2008).

Comfortable energy-efficient behavior would be to predict what is happening on the road ahead and avoid hard braking, drive at the optimal steady speed, and slowly decelerate at stops (Kamal et al., 2013). Recently, several efficient driving systems with the different perspectives, e.g., maximizing energy efficiency, smoothing traffic flows, and improving traffic capacity, have been developed for automated or semi-automated vehicles (Kamal et al., 2013; Sciarretta et al., 2015; HomChaudhuri et al., 2016; Kamal et al., 2014). These systems determine input acceleration using a model predictive control (MPC) framework by solving an optimization problem, which includes the estimated future state of the preceding vehicle in the decision making, and hence, the solution of the problem provides an anticipatory car following behavior that improves the driving efficiency of a vehicle. In contrast, the traditional car following models or ACC decides a control input only

based on the current state of the preceding vehicle, and hence, they cannot avoid aggressive braking or inefficient driving decisions in a transient traffic flow condition. Although the optimal car following scheme improves the driving efficiency of a vehicle, the high computational cost in solving a complex optimization problem reliably and the necessity of powerful computing systems are the main barriers in implementing them on the road vehicles. Therefore, the use of these efficient driving systems remains limited mostly in the simulation studies.

Addressing the above potentials and limitations of the optimal car following schemes, this paper proposes a *look-ahead car following* scheme that is comparable with the traditional car following model in terms of computation cost and reflects the desired anticipatory driving behavior similar to the optimal car following schemes to some extent. Particularly in this paper, the distinctive features of an optimal car following scheme over a traditional car following model of a human driver are investigated. Next, the proposed car following scheme is formulated using a simple mechanism of incorporating the short-term predicted state of the preceding vehicle with a car following model. The suitable predicted horizon or look-ahead time is then chosen through simulation of a vehicle that follows a preceding vehicle according to the real driving data. Finally, the potentials of the proposed scheme are investigated by implementing it on multiple vehicles on roads with signalized intersections. The overall fuel-saving and flowing behavior at intersections by the vehicles with the proposed scheme are evaluated.

2. CAR FOLLOWING SCHEMES

Consider a host vehicle (HV) driving problem where the control acceleration needs to be computed in order to maintain a safe distance from the preceding vehicle (PV) for a given desired speed. Let $x_h = [p_h, v_h] \in \mathbb{R}^2$ denote the state of the HV, where p_h and v_h are the position and velocity, respectively. The control input a_h is given in the form of acceleration. The state dynamics of the HV in a discrete-time framework can then be given by

$$x_h(k+1) = Ax_h(k) + Ba_h(k), \quad (1)$$

where k denotes the step number and, with step size $\Delta\tau$, the coefficient matrices are defined as

$$A = \begin{bmatrix} 1 & \Delta\tau \\ 0 & 1 \end{bmatrix}, \quad B = \begin{bmatrix} 0.5\Delta\tau^2 \\ \Delta\tau \end{bmatrix}. \quad (2)$$

The longitudinal motion of the HV depends on the control input a_h , which is determined by a car following model or automated driving system.

2.1 Traditional Car Following Model

In the case of human driving, we refer it to traditional car following (TCF), it is assumed that the acceleration a_h depends on the states x_h and x_p of the HV and the PV, respectively, and can be represented by a function f_{TCF} as

$$a_h(k) = f_{\text{TCF}}(x_h(k), x_p(k)). \quad (3)$$

The details of the function f_{TCF} can be given according to the equations of any car following model, e.g., Gipps model, OVM or IDM. The Gipps model derives acceleration based on complex safety considerations with

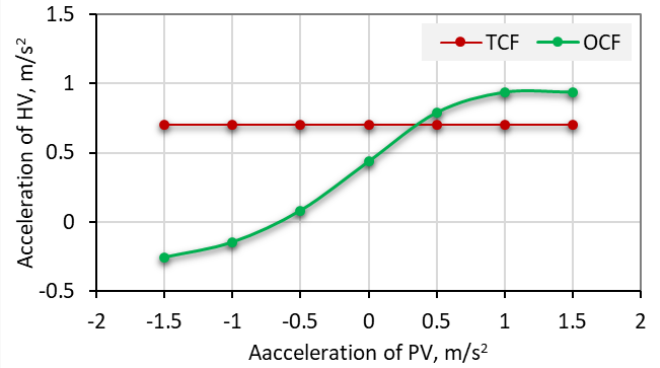


Fig. 1. Generated acceleration of the HV by the TCF and OCF for different acceleration of the PV.

the preceding vehicle. The OVM replicates shock-waves in traffic that often found on the freeways. However, the OVM often produces unrealistic acceleration/deceleration since the relative speed of the preceding vehicle is ignored in deciding acceleration. The intelligent driver model (IDM) (Treiber et al., 2000), a recent and widely used car following model, uses a few model parameters that have clear meanings in the context of traffic flows, provides acceleration as a smoothly varying quantity and ensures collision free driving. The IDM with modified parameters have also been tested for ACC system and found to be effective in improving traffic flows (Kesting et al., 2008). In this study, f_{TCF} is described by the IDM, which is expressed as

$$f_{\text{TCF}}(x_h, x_p) = c_1 \left(1 - \left(\frac{v_h}{\nu} \right)^4 - \left(\frac{d_{\text{hp}}^*}{d_{\text{hp}}} \right)^2 \right), \quad (4)$$

where $d_{\text{hp}} = p_p - p_h$ denotes the distance to the PV, $d_{\text{hp}}^*(v_h, v_p)$ denotes the desired safe distance defined as

$$d_{\text{hp}}^* = s_0 + v_h T + v_h(v_h - v_p)/(2\sqrt{c_1, c_2}), \quad (5)$$

and T, c_1, c_2, s_0, ν are the parameters whose values typically vary among drivers depending on their skills, preferences and unknown factors.

2.2 Optimal Car Following Scheme

A typical car following based on solution of an optimization problem using a MPC framework is briefly described. For simplicity, such driving is refer to optimal car following (OCF) scheme. It is assumed that acceleration of the HV can be determined by anticipating the state of both the HV and the PV according to some given objective function, and such an OCF scheme simple expressed here by a function f_{OCF} as

$$a_h(k) = f_{\text{OCF}}(x_h(k), x_p(k), \bar{a}_p(k)), \quad (6)$$

where $\bar{a}_p(\cdot)$ denotes the estimated acceleration of the preceding vehicle. Specifically, the optimal car following decision can be obtained as

$$f_{\text{OCF}}(x_h(k), x_p(k), \bar{a}_p(k)) = a_h^*(0|k), \quad (7)$$

where $a_h^*(0|k) \in \mathcal{A}^*(k)$ is the immediate control input and $\mathcal{A}^*(k) = [a_h^*(0|k), a_h^*(1|k), \dots, a_h^*(N-1|k)] \in \mathbb{R}^N$ is the optimal input vector obtained as the solution of the following optimization problem at step k :

$$\min_{\mathcal{A}} J(x_h(0|k), \tilde{X}_p(k), \mathcal{A}(k)), \quad (8)$$

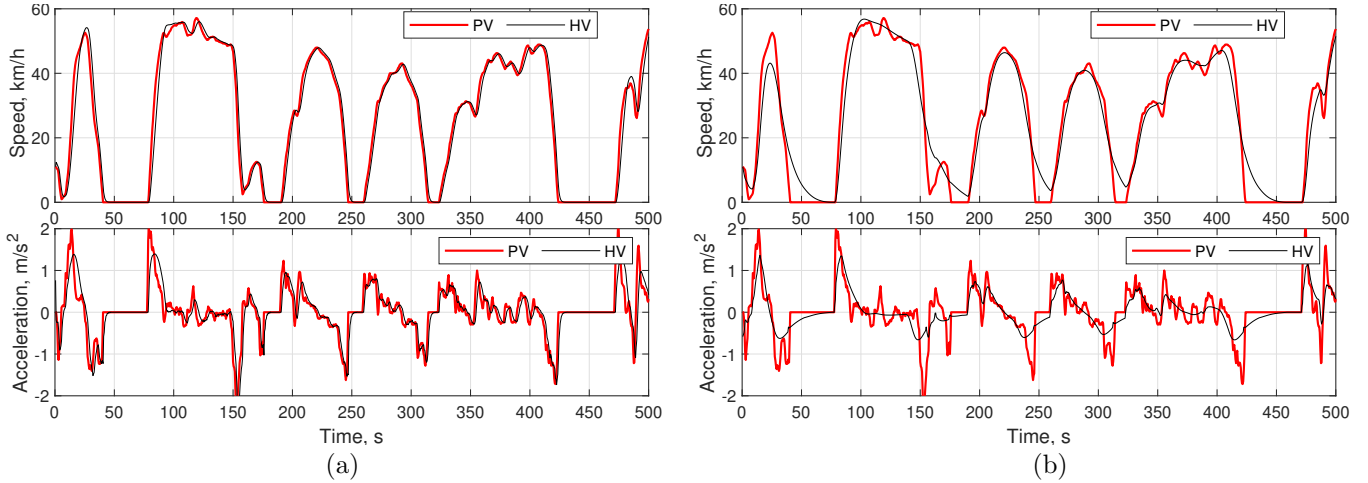


Fig. 2. Speed and acceleration of the HV while following the PV. Using (a) TCF, and (b) the OCF by the HV.

subject to, for $n = 0, 1, 2, \dots, N - 1$, state equations

$$\begin{cases} x_\alpha(0|k) = x_\alpha(k), \alpha \in \{h, p\}, \\ x_\alpha(n+1|k) = Ax_\alpha(n|k) + Ba_\alpha(n|k), \alpha \in \{h, p\}, \end{cases} \quad (9)$$

and constraints

$$\begin{cases} 0 \leq v_h(n+1|k) \leq v_{\max}, \\ a_{\min} \leq a_h(n|k) \leq a_{\max}, \\ p_h(n|k) \leq \tilde{p}_p(n|k) - R_0 - t_0 v_h(n|k), \end{cases} \quad (10)$$

where $v_{\max}, a_{\min}, a_{\max}, R_0, t_0$ are constants, and

$$\tilde{X}_p(k) = [\tilde{x}_p^T(1|k), \tilde{x}_p^T(2|k), \dots, \tilde{x}_p^T(N|k)]^T$$

is the state of the PV in the horizon. Here, $\tilde{X}_p(k)$ is either given (e.g., using vehicle-to-vehicle communication) or can be estimated using both $x_p(k)$ and $\tilde{a}_p(k)$ according to some short-term traffic prediction methods, e.g., conditional persistent prediction (Kamal et al., 2013; Kamal et al., 2018). Basically, at each step k the optimal control inputs $\mathcal{A}^*(k)$ is obtained to control the vehicle along the horizon. However, only the first input $a_h^*(0|k) \in \mathcal{A}^*(k)$ is applied by dismissing the remaining in the vector, and the process is repeated.

Most importantly, the performance index of this optimization problem is defined as

$$\begin{aligned} J(x_h(0|k), \tilde{X}_p(k), \mathcal{A}(k)) = & \sum_{n=1}^N ((V_d - v_h(n|k))^2 + \\ & + \beta_1 a_h^2(n-1|k) + \beta_2 C(x_h(n|k), \tilde{x}_p(n|k))), \end{aligned} \quad (11)$$

where β_1 and β_2 are constant coefficients, V_d, v_h are the desired speed, current speed of the HV, respectively, and $\tilde{x}_p(n|k)$ is the estimated state of the PV, the nonlinear function C denotes penalty when the time headway reduces from the desired value while following the PV, and the function is defined as

$$C(x_h(k), \hat{x}_p(k)) = e^{-\beta_3(t_{d,\min} - t_h(k))}, \quad (12)$$

where $t_{d,\min}$ is the desired minimum time headway, $t_h = (p_p - p_h)/(v_h + \epsilon)$ is the time headway, ϵ is a constant added to avoid singularity at $v_h = 0$. Minimization of the above cost function (11) can ensure efficient and smooth driving (with minimum acceleration and steady speed), and as a consequence of that fuel efficiency of the vehicle is expected to improve.

2.3 Comparison of TCF and OCF

The driving performances of the TCF and the OCF schemes are compared through simulation in two steps by using the typical value of the parameters of the respective schemes. At first, a simple evaluation is conducted in a typical situation where the HV with speed 35 km/h follows a PV with 40 km/h at a gap of 20 m. In this test, for different levels of acceleration of the PV, the calculated acceleration of the HV is shown in Fig. 1. Regardless of the levels of acceleration of the PV, the TCF provides the same acceleration for the HV. However, in the case of the OCF, acceleration of the HV increases with the acceleration of the PV and vice versa. It implies that the OCF predicts the PV and takes advance action to improve its speed or to avoid sudden braking later, which indirectly improves the fuel consumption of the vehicle.

Next, we used real driving data of a vehicle driven at about 7.74 km in about 15 min on National Road 129, Kanagawa, Japan. By setting the PV to follow the real driving pattern exactly, the HV is initialized at the nominal distance with the same speed of the PV. Fig. 2 (a) shows the speed and acceleration of the PV and the HV that are simulated using the TCF. The HV with the TCF shows a speed and acceleration patterns very similar to the PV. Fig. 2 (b) shows the speed and acceleration of the HV driven by the OCF scheme. The HV with the OCF usually avoids any aggressive acceleration or deceleration and keeps the speed smoother than that of the TCF or the PV. It is found that the total fuel consumption by the TCF and the OCF vehicles are 487.9 ml and 459.8 ml, respectively. The anticipation of the PV enables the OCF vehicle in saving about 6% fuel consumption.

The OCF scheme using MPC provides the best driving solution since the control inputs are computed to minimize the driving cost in a given horizon while ensuring various constraints. However, the computation cost is very high compared with the simple car following models. Particularly, the TCF requires less than 0.5 ms to generate the control inputs, whereas the OCF requires above 100 ms using MATLAB in a typical PC. Furthermore, it is very difficult to evaluate a large traffic network containing thousands of vehicles with the existing OCF in real time.

Therefore, it is desired to develop a new car following scheme that can partly reflect the desirable features of the OCF while keeps the computation cost negligible.

3. LOOK-AHEAD CAR FOLLOWING SCHEME

The key difference of the OCF over the TCF is the consideration of the predicted future states of the PV to make an anticipatory control decision. Considering that fact, here we propose a novel way of incorporating the predicted future state of the PV in the parameterized car following model, which we named *Look-ahead Car Following* (LCF) scheme. In this scheme, for a short look-ahead horizon the states of the PV are predicted. Considering the current speed of the host vehicle as constant in the same horizon, the relative look-ahead state of the PV is used in calculating the control input. For a look-ahead horizon $t_{la}|_k$ at step k the LCF, denoted by function f_{LCF} , is formally defined as

$$\begin{aligned} a_h(k) &= f_{LCF}(x_h(k), x_p(k), \bar{a}_p(k)) \\ &= f_{TCF}(\bar{x}_h(t_{la}|_k), \bar{x}_p(t_{la}|_k)) \\ &= a \left(1 - \left(\frac{\bar{v}_h(t_{la}|_k)}{\nu} \right)^4 - \left(\frac{\bar{d}_{hp}^*(t_{la}|_k)}{\bar{d}_{hp}(t_{la}|_k)} \right)^2 \right), \end{aligned} \quad (13)$$

where $\bar{x}_h(t_{la}|_k)$ and $\bar{x}_p(t_{la}|_k)$ are the look-ahead states, $\bar{v}_h(t_{la}|_k)$, $\bar{v}_p(t_{la}|_k)$, $\bar{d}_{hp}(t_{la}|_k)$, $\bar{d}_{hp}^*(t_{la}|_k)$ are the look-ahead values of the variables, which are estimated as

$$\begin{aligned} \bar{v}_h(t_{la}|_k) &= v_h(k), \\ \bar{v}_p(t_{la}|_k) &= v_p(k) + \bar{a}_p(k)t_{la}, \\ \bar{d}_{hp}(t_{la}|_k) &= d_{hp}(k) + (v_p(k) - v_h(k))t_{la} + 0.5a_p(k)t_{la}^2, \\ \bar{d}_{hp}^*(t_{la}|_k) &= s_0 + v_h(k)T \\ &\quad + v_h(k)(v_h(k) - \bar{v}_p(t_{la}|_k))/(2\sqrt{ab}). \end{aligned} \quad (14)$$

The look-ahead horizon t_{la} is dynamically tuned as

$$t_{la} = \begin{cases} H\beta^{-1}v_h, & \text{if } v_h \leq \beta, \\ H, & \text{otherwise,} \end{cases}$$

where β is a constant and H is the maximum look-ahead horizon in second. Depending on speed v_h , the look-ahead horizon t_{la} is tuned linearly from 0 to H when the speed varies from 0 to β . Such tuning at a low speed helps avoiding any oscillatory decision due to the presence of the PV at a short distance.

4. SIMULATION RESULTS

The proposed look-ahead car following scheme has been evaluated through numerical simulation. Using a few scenarios the scheme has been compared with both the OCF and the TCF. For designing the look-ahead parameters for the scheme, the influences of H on the generated acceleration and fuel consumption of a vehicle are observed as follows. At first the control inputs generated by the LCF schemes with different look-ahead horizon H are compared for the case presented in Fig. 1. As stated, acceleration of the PV is varied from -1.5 m/s^2 to 1.5 m/s^2 , and the corresponding control input of the HV is calculated by the proposed LCF scheme for the maximum look-ahead horizon (H) of 0.5 s, 1.0 s and 1.5 s, and compared with the OCF and the TCF as shown in Fig. 3. The

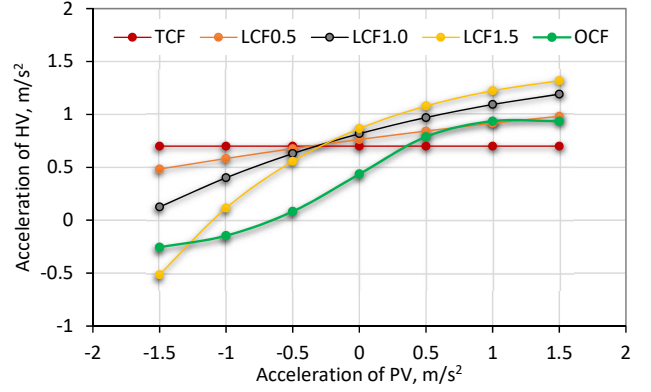


Fig. 3. Acceleration of the HV by the proposed LCF scheme with different look-ahead horizon as the acceleration of the PV varies.

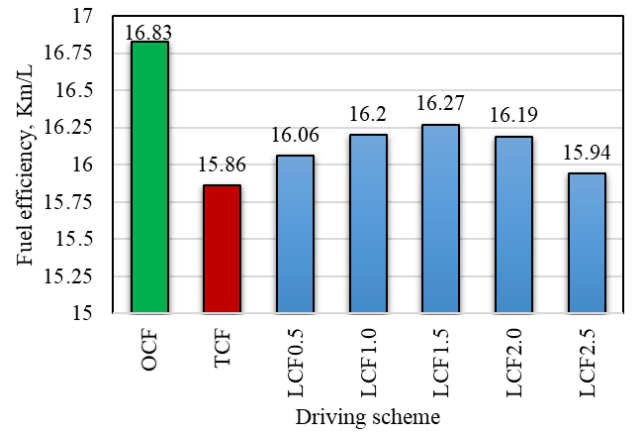


Fig. 4. Overall fuel consumption performance of the HV for different look-ahead horizon of the LCF, and comparison with the OCF and the TCF.

LCF schemes generate higher or lower control input when the PV accelerates or decelerates, respectively, and the difference margin increases with the look-ahead horizon. In this respect, the LCF schemes are more similar to the MCP-based OCF scheme than the TCF. Note that in LCF, it is assumed that the PV would continue the same acceleration over the look-ahead horizon, and at high deceleration of the PV it generates a large negative control input. However, once the HV successively executes the LCF scheme, it would make early adjustment in its relative states, and high negative control input would not be necessary.

The best look-ahead horizon for the LCF schemes need to be determined. For this purpose, by varying the look-ahead horizon, the HV is controlled behind a car that runs according the experimental driving data as shown in Fig. 2. Figure 4 shows the fuel efficiency of the HV for traveling a distance of about 7.74 km in about 15 min. It is found that the LCF with 1.5 s horizon provides the best fuel efficiency, although it is much lower than the OCF scheme, which used the exact future trajectories of the PV in the decision making. The LCF with 1.5 s horizon improves the fuel efficiency by 2.5% compared with the TCF for the same parameters of the car following model. At the higher horizon than 1.5 s, the fuel efficiency deteriorates

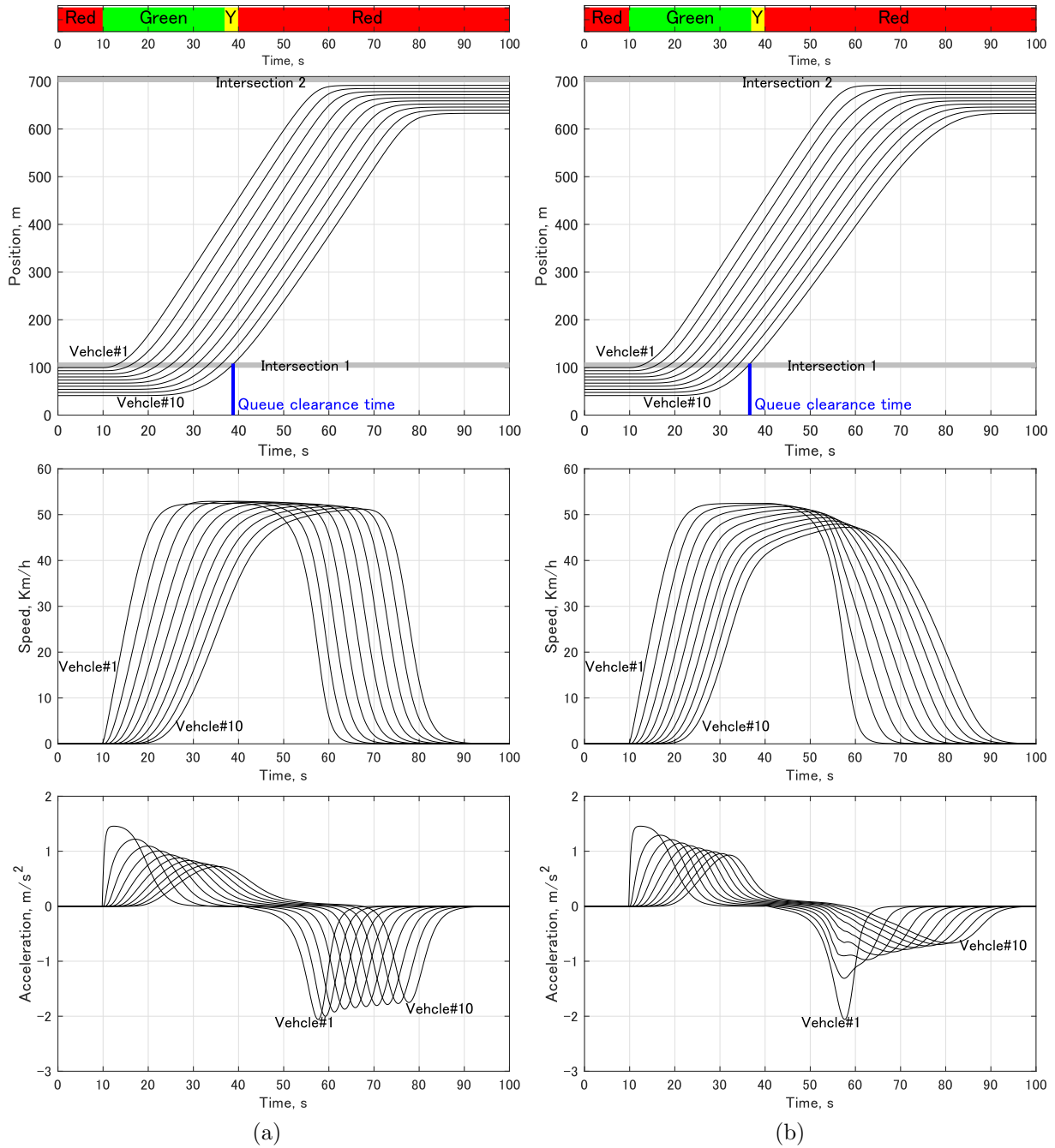


Fig. 5. Driving characteristics while leaving the queue at the green signal appearance and stopping at the red signal in the intersections by ten vehicles driven by (a) TCF and (b) LCF.

since large horizon often causes fluctuating control inputs due to variation in the speed of the PV. Therefore, the LCF with $H = 1.5$ s with $\beta = 4$ m/s is chosen for the subsequent simulation.

Possible impacts on the traffic flow by the proposed LCF scheme have been evaluated by observing the driving characteristics of a string of ten vehicles at intersections as shown in Fig. 5. More specifically, trajectories, speeds, and accelerations of these vehicles are observed while they leave a queue at the first intersection and travel to another intersection separated by 700 m and having the red signal. Initially, ten vehicles in the queue are idling due to the red signal, which turns into the green at time

10 s. The signals of both consecutive intersections are synchronized for simplicity, and the red signal appears again at time 40 s and continues up to 100 s. The LCF vehicles apply slightly higher acceleration and speed up a bit faster than the vehicles with the TCF. In contrast to the start-up characteristics, during stopping at the red signal, the LCF vehicles use significantly low deceleration in a very anticipative manner. Such smooth deceleration ensures better utilization of kinetic energy to save fuel consumption and reduce emissions. A similar comparison between TCF and OCF can be found in Bakibillah et al. (2019).

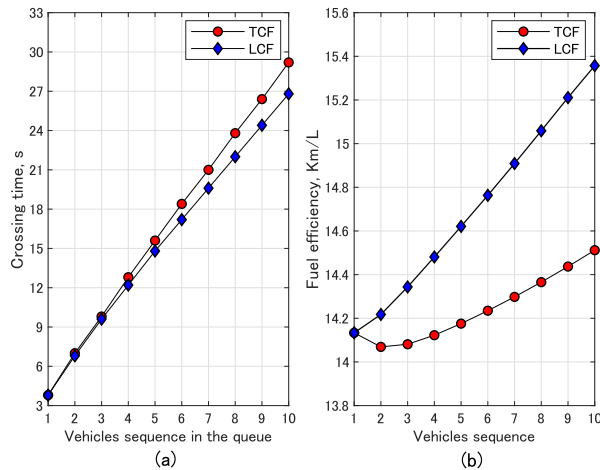


Fig. 6. Improvements in traffic performance: (a) intersection crossing time, and (b) fuel efficiency.

Finally, the queue clearing timings and fuel consumption efficiency in the observed period are evaluated for each of these vehicles in Fig. 6. The leading vehicle left the intersection typically, while the 2nd to the 10th vehicles follow their respective PV. Vehicles with the LCF cross the intersection slightly faster than the TCF vehicles as shown in Fig. 6 (a), e.g., the 10th vehicle could cross 2.4 s earlier. This implies that the LCF reduces the start-up delays of the vehicles that directly enhances the capacity of the intersection. Considering the 90 s cycle with the two-phase signal in the intersection, it improves the effective green time by 5.3% that directly relates the capacity enhancement of the intersection. Fig. 6 (b) shows the average fuel efficiency of these vehicles in both cases. Since the total travel distance of the vehicles slightly differs, we have shown the fuel consumption rate in km/L for a fair comparison. By starting up faster and stopping slower, the LCF vehicles significantly improve fuel consumption efficiency. The improvement margin of the 10th vehicle is the highest since it could decelerate for the longest distance by better utilizing the kinetic energy. These achievements illustrate the potentials of the proposed LCF in improving both the traffic flows and fuel efficiency.

5. CONCLUSIONS AND FUTURE WORK

In this paper, a look-ahead car following scheme has been proposed that can partly reflect the desired driving characteristics usually obtained from the solution of the optimization problem. The proposed scheme reduces the start-up delays of the traffic in the queue departure at the intersection and significantly improves the effective green time, and hence, enhances the intersection capacity. Furthermore, it attempts to decelerate slowly while stopping at intersections, and such behavior helps to improve fuel efficiency by utilizing the kinetic energy.

In the future, we would also like to investigate the impacts of the LCF scheme in a urban and freeway networks.

ACKNOWLEDGEMENTS

This research is supported by JSPS Grant-in-Aid for Scientific Research (A) 18H03774.

REFERENCES

- Bakibillah, A.S.M., Hasan, M., Rahman, M.M., and Kamaal, M.A.S. (2019). Predictive car-following scheme for improving traffic flows on urban road networks. *Control Theory and Technology*, 17(4), 325–334.
- Bando, M., Hasebe, K., Nakayama, A., Shibata, A., and Sugiyama, Y. (1995). Dynamical model of traffic congestion and numerical simulation. *Physical Review E*, 51(2), 1035–1042.
- Berry, I.M. (2010). *The effects of driving style and vehicle performance on the real-world fuel consumption of US light-duty vehicles*. Ph.D. thesis, Massachusetts Institute of Technology.
- Brackstone, M. and McDonald, M. (1999). Car-following: a historical review. *Transportation Research Part F: Traffic Psychology and Behaviour*, 2(4), 181–196.
- Davis, L. (2004). Effect of adaptive cruise control systems on traffic flow. *Physical Review E*, 69(6), 066110.
- Gipps, P.G. (1981). A behavioural car-following model for computer simulation. *Transportation Research Part B: Methodological*, 15(2), 105–111.
- HomChaudhuri, B., Vahidi, A., and Pisu, P. (2016). Fast model predictive control-based fuel efficient control strategy for a group of connected vehicles in urban road conditions. *IEEE Transactions on Control Systems Technology*, 25(2), 760–767.
- Kamal, M.A.S., Mukai, M., Murata, J., and Kawabe, T. (2013). Model predictive control of vehicles on urban roads for improved fuel economy. *IEEE Transactions on Control Systems Technology*, 21(3), 831–841.
- Kamal, M.A.S., Hayakawa, T., and Imura, J.i. (2018). Road-speed profile for enhanced perception of traffic conditions in a partially connected vehicle environment. *IEEE Transactions on Vehicular Technology*, 67(8), 6824–6837.
- Kamal, M.A.S., Imura, J.i., Hayakawa, T., Ohata, A., and Aihara, K. (2014). Smart driving of a vehicle using model predictive control for improving traffic flow. *IEEE Transactions on Intelligent Transportation Systems*, 15(2), 878–888.
- Kesting, A., Treiber, M., Schönhof, M., and Helbing, D. (2008). Adaptive cruise control design for active congestion avoidance. *Transportation Research Part C: Emerging Technologies*, 16(6), 668–683.
- Knowles, M., Scott, H., and Baglee, D. (2012). The effect of driving style on electric vehicle performance, economy and perception. *International Journal of Electric and Hybrid Vehicles*, 4(3), 228–247.
- Koonce, P., Rodegerdts, L., Kevin, L., Quayle, S., Beaird, S., Braud, C., Bonneson, J., Tarnoff, P., and Urbanik, T. (2008). Traffic signal timing manual. Technical Report FHWA-HOP-08-024, U.S. Department of Transportation, Federal Highway Administration.
- Sciarretta, A., De Nunzio, G., and Ojeda, L.L. (2015). Optimal ecodriving control: Energy-efficient driving of road vehicles as an optimal control problem. *IEEE Control Systems Magazine*, 35(5), 71–90.
- Treiber, M., Hennecke, A., and Helbing, D. (2000). Congested traffic states in empirical observations and microscopic simulations. *Physical Review E*, 62(2), 1805–1824.